TECTONICS, VOL. 7, NO. 3, PAGES 563-582, JUNE 1988

CONTINENTAL EROSION AND LARGE-SCALE RELIEF

Patrick Pinet and Marc Souriau

Groupe de Recherche de Géodésie Spatiale,
Centre National d'Etudes Spatiales,
Toulouse, France

Abstract. A worldwide investigation of continental erosion is carried out by the study of large drainage basins, on the basis of hydrological data, environmental factors, and basin relief distribution. Inside each basin, mean geochemical and mechanical denudation rates are defined. A multicorrelation analysis shows that the mechanical denudation rates Ds are uncorrelated with environmental factors and correlated with mean basin elevation H, while chemical denudation rates Dd are insensitive to relief but correlated with mean annual precipitation. Furthermore, two linear relationships between H and Ds are detected: (1) Ds ($m/10^3$ yr) = 419 x 10^{-6} H (m) - 0.245, with V (explained variance) = 95.1%; this law concerns basins related to orogenies younger than 250 Ma. The negative intercept is interpreted as a continental sedimentation rate of 245 m/m.y. An alternative model in which one invokes a critical elevation, separating erosion from sedimentation, is equally successful and leads to lower sedimentation rates (60-110 m/m.y.). For both models, one derives from the slope of the adjustments, erosion time constants on the order of 2.5 m.y. (2) Ds ($m/10^3$ yr) = 61 x 10^{-6} H (m), with V = 86.5%; this law concerns basins related to older orogenies. The null intercept suggests the lack of continental storage. Because of the more important dispersion of the data, the erosion time constant is calculated separately for each basin; it ranges from 15 to 360 m.y. The tectonic implications of these results are discussed. In particular, the short time constant 2.5 m.y. agrees with orogenic uplift rates on the order of 1 mm/yr, observed in active mountain chains.

Paper number 7T0908.
0278-7407/88/007T-0908$10.00

INTRODUCTION

In the field of geomorphology, many investigations have been devoted to the study of denudation processes in relation to the relief and other environmental factors such as climate (precipitation, temperature, etc.). Denudation processes are evaluated by two different methods; the most direct one consists in the measurement of the rate of ground lowering [Ruxton and McDougall, 1967]; the other one starts from river sediment yields and converts them into mean denudation rates [Schumm, 1963; Ahnert, 1970]. However, these studies focused on local or regional features of the landscape, and it is hazardous to extrapolate them to large areas. Here, we intend to concentrate on large spatial scales governed probably by long time

constants, following in this approach, the emerging concepts of global megageomorphology [NASA, 1985]. We think that, at such a scale, the relationship of drainage to tectonism is of particular concern. Specifically, this work is an attempt to detect global patterns, in particular, worldwide relationships between denudation rate, derived from river sediment delivery, and relief of the main hydrographic basins.

However, earlier studies [Langbein and Schumm, 1958; Fournier, 1960; Corbel, 1964; Judson and Ritter, 1964; Wilson, 1973; Jansen and Painter, 1974] have suggested that denudation processes are influenced by various parameters such as geometry, hydrology, and climatic conditions of the drainage basin; the sensitivity of the denudation rates to such environmental factors must be tested, before invoking relief as the main parameter.

RATIONALE OF ANALYSIS

The study of Ruxton and McDougall leads from direct estimates of local denudation rates on the slopes of a 650,000-year-old andesite stratovolcano in New Guinea, to the linear relationship

$$- dh/dt = k \cdot h \qquad (1)$$

where h is the local elevation.

The indirect method [Schumm, 1963; Ahnert, 1970] derives, from annual river sediment yields Ms, mean denudation rates Ds for the whole drainage basins defined as follows: $Ds = Ms/\rho.A$, where ρ is the standard rock density and A is the basin area. Schumm considers small drainage basins on the order of 4000 km^2 and obtains the following exponential relationship between mean denudation rate Ds and mean elevation H (normalized by the basin length):

$$\log Ds \text{ (feet/1000 yr)} = 26.866\ H - 1.7238$$

while Ahnert looks at 20 mid-latitude medium-sized drainage basins ranging from about 1000 to 100,000 km^2, located in the United States and Western Europe, and obtains a linear relationship between Ds and H. It is shown in the present study that any exponential relationship between denudation and relief does not fit our data set. Thus, let us consider

$$Ds = K \cdot H \qquad (2)$$

where

$$H = 1/A \int_A h \cdot dA$$

If one assumes

$$Ds = -1/A \int_A dh/dt \cdot dA = - dH/dt$$

then

$$- dH/dt = K \cdot H \qquad (3)$$

The comparison between K and k values will show whether the denudation process is homogeneous at all spatial scales. The solution of (3) is

$$H(t) = Ho \exp (- t/\tau) \qquad (4)$$

where $\tau = 1/K$. We will refer to as the erosion time constant in the following and compare it to the values obtained, on one hand, by Ruxton and McDougall, on the order of 1 m.y., and, on the other hand, by Ahnert, around 6 m.y.

It is worth noting that, in this approach, any proposed functional relationship between denudation process and relief will concern the largest wavelengths of the elevation distribution within each basin as we deal with the mean basin elevation.

Equation (3) implies that no deposition takes place above sea level. Then the denudation rate Ds can be identified as the mean erosion rate. However, cases of sediment storage inside watersheds are well documented [Trimble, 1977, 1982, 1983], so that some denudation rates may underestimate the erosion processes. Consequently, in a second step, models taking into account a global sedimentation component in the basin are tested, and the implications discussed.

DATA AND METHOD

Denudation rates are derived from the total sediment load in the rivers. This load is considered as the sum of dissolved and suspended loads with an additional bedload. Suspended and dissolved sediment loads are studied separately, as they have mechanical and chemical origins, respectively. Bedload is not taken into account, as too few high-quality data are presently available. It is commonly assumed to comprise less than

about 10% of the total load, but may occasionally be important [Peters, 1978; Chorley et al., 1984].

Recently, available data concerning major drainage basins all over the world [Milliman and Meade, 1983; Meybeck, 1985] allow for a continental scale investigation. If one considers continents as composed of independent surface subunits defined by the major drainage basins, then the mean sediment yield, measured at the mouth of the largest rivers, gives access to the mean denudation rate inside the basin and consequently, if global erosion is controlled by the rivers, to continental erosion at broad scale, being aware that continental sedimentation is not excluded [Walling, 1983; Trimble, 1983; Meade and Parker, 1985].

Suspended sediment loads mainly come from the compilation of river data by Milliman and Meade [1983] while dissolved loads are taken from Meybeck [1985].

In order to look for linear functional relationships between the main environmental factors and denudation, we establish for 45 major drainage basins a global set of the following raw data: Main stream length L, basin area A, annual suspended sediment load Ms, annual dissolved sediment load Md, annual water discharge W, mean elevation H, mean annual precipitation P, and mean annual temperature T.

These data are summarized in Table 1, and the location of these basins is shown in Figure 2. The basin areas are obtained by digitizing the basin contours following the divides on the world map of the IGN [1968]. Our basin area determinations are in general agreement with earlier estimates [UNESCO, 1972, 1974, 1979], except for some poorly delimited basins in arid regions, such as the Nile. The superimposition of these contours on the map compiled by the National Center for Atmospheric Research [1982] provides us with the mean elevation of the basin topography.

The main stream length, mean annual precipitation, and temperature estimates at the basin scale are derived from Encyclopedia Britannica [1969, table p. 276; maps pp. 144, 142, 143].

The hydrological data (Ms, W) are mainly taken from the recent budget of Milliman and Meade [1983], except for some rivers such as the Nile, Colorado, Columbia, Zambezi, Mississippi, and Indus for which the recent data are deeply altered by the edification of dams. Earlier data have thus been considered from Holeman [1968] for the Nile, Colorado, and Indus, from Lisitzin [1972] for the Mississippi and Zambezi, from Judson and Ritter [1964] for the Columbia. Besides, the Ms estimate for the Niger in the work by Milliman and Meade [1983] is from NEDECO [1959] and is underestimated; we take here the estimate from Lisitzin [1972]. For the Tigris/-Euphrates basin, no recent Ms estimate is available; we adopt that of Holeman [1968]. Also, in the case of the Orange river, a drastic change in the lithology during the last 50 years [Milliman and Meade, 1983] has driven us to take an earlier estimate (cf. Table 1). However, as mentioned by Milliman and Meade [1983], these data have a widely variable quality, due to differences in the measurement techniques, in the length of observation and in the sampling procedures. In addition, the data have sometimes been collected at gaging stations far upstream from the river mouth, and the sediment yield estimate may be erroneous. Consequently a global processing of these data is necessary in order to smooth out the measurement errors, and on this basis, the dubious cases will be rejected eventually in the course of the analysis.

A difference in the water discharge estimate W of the Nile is also noted between the estimate W = 30 km^3/yr of Milliman and Meade [1983] from UNESCO [1972, 1974, 1979] and W = 89 km^3/yr in the compilation by Meybeck [1976] from the Food and Agriculture Organization (FAO) [1971]. The earliest estimate is arbitrarily taken here.

Also, the annual dissolved sediment load Dd is given for 27 out of the 45 basins studied here and comes from the recent compilation by Meybeck [1976] revised in 1985.

From these data, we derive, for each basin, mean denudation rates Ds, Dd and the runoff Dw (or specific discharge) as follows: $Ds = Ms/\rho \cdot A$, $Dd = Md/\rho \cdot A$, $Dw = W/A$ with $\rho = 2500\ kg/m^3$.

RESULTS

Multicorrelation Analysis

A multicorrelation analysis is performed on the global data set of the following nine variables (L, A, M*, W, Dw, H, P, T, D*) (where (M*, D*) are successively

TABLE 1. Geometry, Hydrological and Climatological Data, Relief and Denudation Rates of 45 Major Drainage Basins in the World

	n°	L, km	10^6A, km^2	10^6Ms, t/yr	10^6Md, t/yr	W, km^3/yr	Dw, cm/yr	P, cm/yr	T, °F	H, m	Dd, $m/10^3$yr	Ds, $m/10^3$yr
Amazon	1	6299	5.908	900	292	6300	106.6	203	80	467	0.0198	0.0609
Zaire	2	4370	3.698	43	47	1250	33.8	152	75	751	0.0051	0.0047
Mississippi	3	3778	3.265	500	131	580	17.8	76	55	661	0.0160	0.0612
Parana	4	4499	2.868	92	56	470	16.4	114	70	557	0.0078	0.0128
Ienissei	5	4129	2.553	13	73	560	21.9	38	20	741	0.0114	0.0020
Lena	6	4269	2.438	12	9	514	21.1	25	15	600	0.0015	0.0020
Ob	7	3680	2.249	16	50	385	17.1	38	30	208	0.0089	0.0028
Amour	8	4352	1.923	52	20	325	16.9	38	30	585	0.0042	0.0108
Nil	9	6689	1.905	111	17.5	89	4.7	51	80	856	0.0037	0.0233
Yangtze	10	5525	1.827	478	166	900	49.3	127	60	1601	0.0363	0.1047
Ganges/ Brahmaputra	11	5401	1.669	1670	323.5	971	58.2	203	65	1535	0.0775	0.4002
Mackenzie	12	4240	1.616	100	70	306	18.9	38	25	618	0.0173	0.0248
Niger	13	4183	1.550	67	10	192	12.4	114	85	364	0.0026	0.0173
Zambezi	14	2735	1.420	100	15.5	223	15.7	102	70	1009	0.0044	0.0056
Murray	15	2589	1.140	30	9	22	1.9	76	65	243	0.0031	0.0105
St. Lawrence	16	3057	1.099	4	54	447	40.7	89	40	271	0.0196	0.0015
Orinoco	17	2061	1.020	210	49	1100	107.8	140	75	373	0.0192	0.0824
Tigris/ Euphrates	18	2800	0.923	53	--	46	5.0	25	70	652	---	0.0230
Indus	19	2896	0.916	440	62	238	26.	38	75	1807	0.0271	0.0437
Mekong	20	4023	0.849	160	60	470	55.4	127	70	875	0.0283	0.0754
Yukon	21	3701	0.833	60	34	195	23.4	38	25	727	0.0163	0.0288
Huangho	22	4668	0.814	1080	33.5	49	6.0	76	55	1860	0.0165	0.5310
Danube	23	2859	0.778	67	60	206	26.5	76	50	501	0.0308	0.0344
Orange	24	2092	0.726	153	1.5	11	1.5	38	60	1240	0.0008	0.0843
Colorado	25	2317	0.715	135	14.5	20	2.8	25	60	1537	0.0081	0.0755
Columbia	26	1850	0.670	29	--	251	37.4	64	50	1293	---	0.0048
Kolyma	27	2599	0.658	6	--	71	10.8	13	15	557	---	0.0037
Sao Francisco	28	3199	0.630	6	--	97	15.4	102	75	614	---	0.0038
Si Kiang	29	1957	0.464	69	132	302	65.0	178	70	670	0.1137	0.0594
Irrawaddi	30	2092	0.414	265	91	428	103.4	178	75	758	0.0879	0.2560
Indigirka	31	1789	0.356	14	--	55	15.4	13	10	713	---	0.0157
Limpopo	32	1770	0.342	33	--	5	1.5	76	70	766	---	0.0386
Godavari	33	1448	0.322	96	--	84	26.1	102	85	413	---	0.1194
Magdalena	34	1537	0.276	220	28	237	85.6	127	75	1203	0.0406	0.3193
Severnaia Dvina	35	740	0.262	5	--	106	40.5	38	35	119	---	0.0069
Fraser	36	1368	0.247	20	--	112	45.4	76	40	1140	---	0.0324
Yana	37	1368	0.240	3	--	29	12.1	13	5	703	---	0.0050
Mehandi	38	1295	0.195	2	--	67	34.3	127	75	330	---	0.0041
Liao He	39	1438	0.191	41	--	6	3.1	76	45	496	---	0.0859
Rufiji	40	1237	0.180	17	--	9	5.0	114	70	912	---	0.0378
Rio Negro	41	729	0.178	13	--	30	16.8	25	60	745	---	0.0292
Hungho	42	1200	0.165	130	--	123	74.7	152	75	987	---	0.3157
Rhone	43	813	0.099	10	--	49	49.4	102	55	754	---	0.0403
Pô	44	652	0.070	15	--	46	65.6	76	55	793	---	0.0860
Susitna	45	600	0.051	25	--	40	78.9	76	30	1031	---	0.1974

Values are given by decreasing basin surface; variables L, A, Ms, Md, W, Dw, P, T, H, Dd, Ds are defined in the text.

TABLE 2a. Correlation Analysis of the Global Set of Data Given in Table 1: Correlation Matrix for Case 1 (Dissolved Sediment Load)

	L	A	Md	Dw	W	H	P	T	Dd
L	1.								
A	0.65	1.							
Md	0.43	0.45	1.						
Dw	-0.13	0.08	0.52	1.					
W	0.43	0.77	0.66	0.54	1.				
H	0.05	-0.29	0.14	-0.10	-0.17	1.			
P	0.08	0.20	0.67	0.76	0.51	-0.03	1.		
T	-0.05	-0.01	0.18	0.37	0.22	0.20	0.63	1.	
Dd	-0.23	-0.32	0.53	0.59	0.02	0.18	0.63	0.25	1.

taken as (Md, Dd) in case 1 (dissolved sediment load) and (Ms, Ds) in case 2 (suspended sediment load). The correlation matrix, for each case, is given in Tables 2a and 2b. We note that water discharge W and basin area A are well-correlated (R (W, A) = 0.76), suggesting that the runoff Dw = W/A is a significant variable. A correlation is also noted between the main stream length L and the basin surface A (R (L, A) = 0.77) in agreement with earlier analyses [e.g., Schumm, 1956].

Case 1: Dissolved sediment load. The correlation analysis between the variables indicates that Dd is mainly correlated with the precipitation (R (P, Dd) = 0.63; confidence interval [0.42-0.76]) or the runoff (R (Dw, Dd) = 0.59; confidence interval [0.32-0.75]), which are strongly interdependent (R (P, Dw) = 0.76), and is not correlated with the basin mean elevation (R (H, Dd) = 0.18).

Although one knows that dissolved sediment load has important atmospheric and human origins and that consequently, only a fraction of the dissolved matter in the rivers comes from the chemical denudation of the continents, one concludes from the above results that the continental chemical denudation is independent of the relief and directly related to the runoff when it is analyzed at a continental scale. Precipitation appears to be the dominant environmental factor. This is in agreement with earlier studies [Meybeck, 1976; Holland, 1978, p. 144].

Case 2: Suspended sediment load. The analysis of the correlation indicates that, apart from the obvious correlation existing between the sediment load and denudation rate, the mechanical worldwide denudation rate is mainly correlated (R (H, Ds) = 0.62; confidence interval [0.42-0.75] with the mean elevation of the major drainage basins and poorly or not correlated with other environmental factors, either hydrological or climatological ones. However, the graph of the

TABLE 2b. Correlation Analysis of the Global Set of Data Given in Table 1: Correlation Matrix for Case 2 (Suspended Sediment Load)

	L	A	Ms	Dw	W	H	P	T	Dd
L	1.								
A	0.77	1.							
Ms	0.49	0.35	1.						
Dw	-0.10	0.08	0.26	1.					
W	0.47	0.76	0.44	0.48	1.				
H	0.12	-0.13	0.50	0.01	-0.10	1.			
P	0.17	0.24	0.46	0.67	0.47	0.04	1.		
T	0.09	0.08	0.24	0.24	0.20	0.14	0.66	1.	
Ds	0.04	-0.17	0.70	0.36	0.00	0.62	0.38	0.26	1.

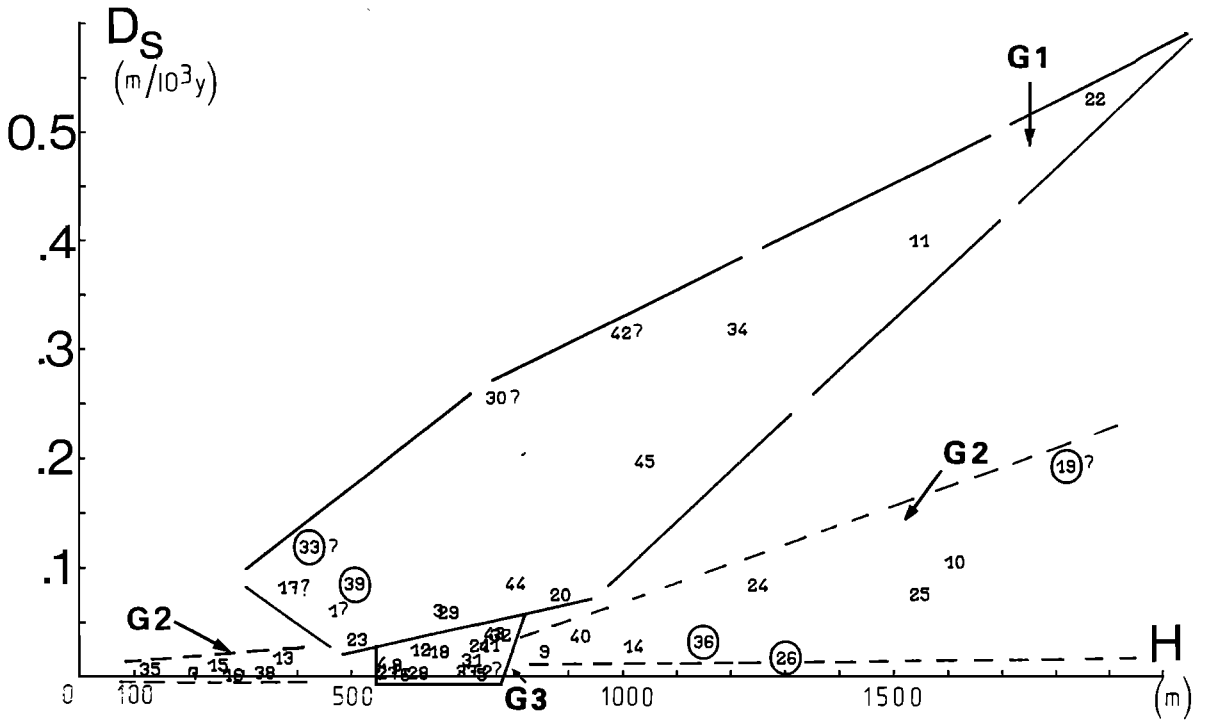

Fig. 1. Graph of the denudation rate Ds ($m/10^3$ yr) versus the mean basin elevation H (m).

denudation rate Ds versus the mean elevation H (Figure 1) shows that the functional relationship is not simple. The following remarks can be made:

1. The obtained pattern cannot be taken into account by simple nonlinear trends; the following nonlinear relationships $Ds = \alpha \cdot H^{\beta}$ and $Ds = \lambda \cdot \exp^{\mu H}$ (α, β, λ, μ constants) have been unsuccessfully tested, excluding the exponential relationship proposed by Schumm [1963].

2. As H increases (H > 800 m), the basin population splits into two distinct groups. Group 1 includes a priori the following basins, characterized by high H and Ds values: (1, 3, 11, 17, 20, 22, 23, 29, 30, 33, 34, 39, 42, 44, 45). Group 2 includes a priori the following basins characterized by lower Ds values: (9, 10, 14, 19, 24, 25, 26, 36, 40).

3. For H < 800 m, we note two points: (1) There is a group of basins which appears as the extension toward low H values of group 2 and is composed of basins n° = 7, 13, 15, 16, 35, 38. (2) There is a clustering of the denudation rate values for 500< H < 800 m; this clustering corresponds to the intersection of the two groups mentioned above and suggests an overdensification of the population due to the mixing of two independent populations. As a hint, this clustering is roughly in between the mean and modal values of both H and Ds variables. This places some ambiguity on the adherence to one or the other group, for the basins belonging to the cluster (2, 4, 5, 6, 8, 12, 18, 21, 27, 28, 31, 32, 37, 41, 43). Finally, we end up with two distinct groups of 15 basins each:

G1 = (1, 3, 11, 17, 20, 22, 23, 29, 30, 33, 34, 39, 42, 44, 45)

G2 = (7, 9, 10, 13, 14, 15, 16, 19, 24, 25, 26, 35, 36, 38, 40)

and a set G3 of 15 basins located at the intersection of the two preceding groups. Dubious denudation rates, based on dubious hydrological estimates (see Milliman and Meade [1983] for a critical analysis), are indicated in Figure 1 by question marks (1, 2, 17, 19, 30, 33, 42); one can check that they have no important bearing on the proposed splitting, as they are distributed randomly on the graph. These groupings

TABLE 3a. Correlation Analysis for Subsets G1 and G2 in Case 2: Correlation Matrix for Group G1

	L	A	Ms	Dw	W	H	P	T	Ds
L	1.								
A	0.77	1.							
Ms	0.82	0.51	1.						
Dw	-0.06	0.18	-0.05	1.					
W	0.64	0.90	0.39	0.44	1.				
H	0.27	-0.18	0.60	-0.15	-0.25	1.			
P	0.42	0.38	0.43	0.65	0.54	0.01	1.		
T	0.21	0.23	0.11	0.42	0.35	-0.20	0.66	1.	
Ds	0.17	-0.22	0.57	-0.05	-0.22	0.90	0.13	0.01	1.

lead to the conclusion that the previous multicorrelation analysis, applied to the global set, concerns two distinct subsets of homogeneous data. Consequently, a second correlation analysis is thus performed on the a priori independent groups G1 and G2 in order to detect potential factors, specific to each group and correlated with the denudation rate Ds; the result is given in Tables 3a and 3b. This analysis makes it evident that H is the dominant factor, and the only one for each separate group (for G1: R (H, Ds) = 0.9 with a confidence interval [0.68-0.96]; for G2: R (H, Ds) = 0.81 with a confidence interval [0.51-0.93]). This means that, basically, the difference between the two observed trends has to be ascribed to a difference in the basin relief itself; this difference may arise from the relief distribution, i.e., from the global basin morphology, and, as the climatic factors do not appear to be involved, it can be due to the tectonic inputs of the drainage basin. Another alternative might be major differences in the lithology, but since our investigation is at very broad scale, this seems unlikely.

The immediate question is thus, what are the common features, in terms of tectonics, of the drainage basins belonging to each group? Looking at a global map of the major tectonic features of the world [Burchfiel, 1983, Figure 6] reveals that the G1 basins are mainly (87%) associated with recent orogenies (less than 250 Ma) while G2 basins are mainly (80%) correlated with much older orogenies. The association (basin-orogeny) may be either complete or partial depending on whether the whole drainage basin or a part of it belongs to the orogenic belt [Potter, 1978]. In G1, the intermediate case corresponds, at various degrees, to 1-Amazon, 3-Mississippi, 17-Orinoco, 22-Huangho, 29-Si Kiang, 42-Hungho basins for which only the spring of the main stream or of the important tributaries is really in the

TABLE 3b. Correlation Analysis for Subsets G1 and G2 in Case 2: Correlation Matrix for Group G2

	L	A	Ms	Dw	W	H	P	T	Ds
L	1.								
A	0.81	1.							
Ms	0.45	0.30	1.						
Dw	-0.14	-0.18	0.15	1.					
W	0.50	0.54	0.55	0.59	1.				
H	0.12	-0.07	0.73	0.03	0.18	1.			
P	0.08	-0.02	-0.01	0.27	0.33	-0.16	1.		
T	0.33	0.08	0.30	-0.47	-0.23	0.24	0.37	1.	
Ds	0.14	0.00	0.89	-0.01	0.20	0.81	-0.23	0.29	1.

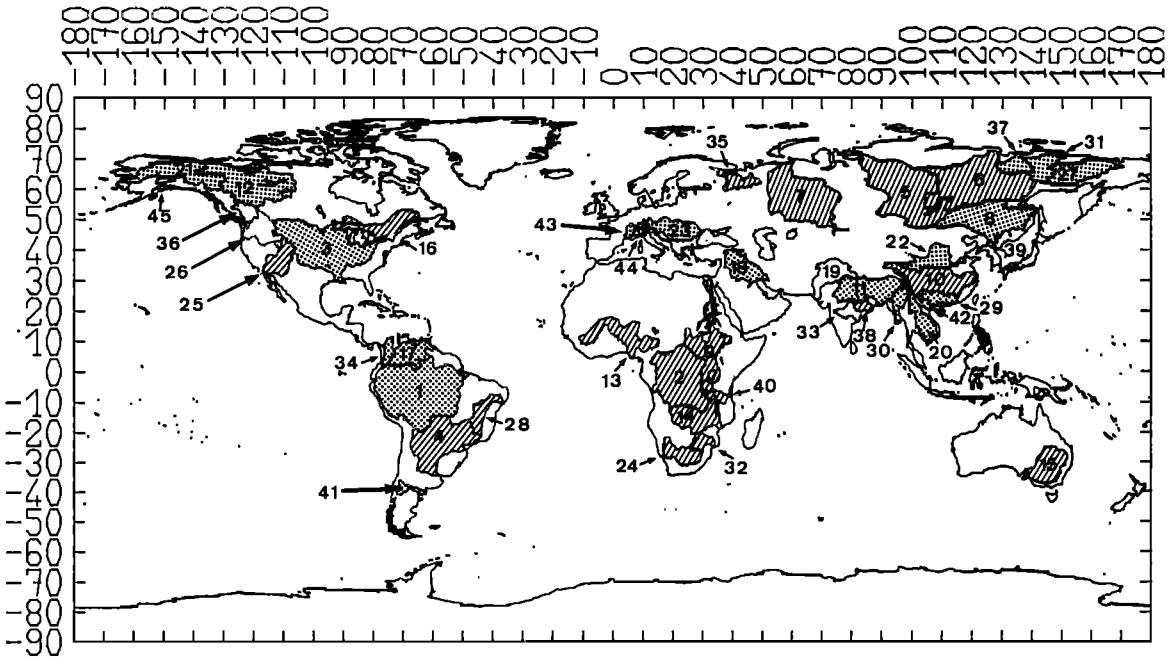

Fig. 2. Location of the 45 major drainage basins considered in Table 1; dotted and hatched areas correspond to basins associated with recent (less than 250 Ma) and older orogenies, respectively; basins in white do not fit the proposed criterion.

recent mountain belt and the major part of the basin spreads out, away from the belt, while 11-Ganges-/ Brahmaputra, 20-Mekong, 30-Irrawaddi, 34-Magdalena, 44-Pô, 45-Susitna basins are "typical" of the pure case. In G2, the Yangtze basin represents an intermediate case; although the Yangtze river flows down from the Himalayas, a large part of the basin (Red basin) lies on an old shield (2.5-0.7 b.y.). However, five basins out of 30 (i.e., 16%) disagree with this general scheme: in G1, two basins (33-Godavari, 39-Liaohe) are located on Precambrian shields, and in G2, three basins are associated with recent orogenies (26-Columbia, 36-Fraser, 19-Indus). Although these partial discrepancies may mean that the criterion proposed above is not an efficient discriminator, they may also simply reflect either particular behaviors due to local conditions (e.g., Columbia and Fraser basins are in the same part of the Rocky mountains) or the inadequacy of the data base (e.g., the Godavari and Indus rivers). On the basis of the proposed discrimination between the drainage basins according to the age of the main associated orogeny, the basins belonging to G3 can be attributed either to G1 or G2. This leads to the following splitting of G3: G3.1 = (8-Amour, 12-MacKenzie, 18-Tigris-Euphrates, 21-Yukon, 27-Kolyma, 31-Indigirka, 37-Yana, 41-Rio Negro, 43-Rhône) and G3.2 = (2-Zaire, 4-Parana, 5-Ienissei, 6-Lena, 28-Sao Francisco, 32-Limpopo) are added to G1 and G2, respectively. The global geographical distribution of these two groups of basins is shown in Figure 2.

Quantitative Linear Regression Analysis

Search for a linear relationship between denudation rate and relief. On the basis of the preceding correlation analysis and of the geologic discrimination proposed above, global linear adjustments between Ds and H are first performed on the sets G1 and G2. Then, we look at the improvement of the statistical criteria (V: percentage of explained variance, σ: standard deviation, d: standard deviation as a percentage of the response mean)

TABLE 4. Regression Laws Ds=K.H+Do for Basins Associated With Recent Orogenies

Group	Number of Basins	K, 10^{-3} yr^{-1}	Do, m/10^3 yr	V, %	σ, m/10^3yr	d, %	Fisher Test Experimental	Fisher Test Theoretical
G1	15	320 x 10^{-6}	-0.090	81.6	0.067	38	57.5	6.7
$G1_H$	10	371	-0.172	94.	0.045	24	127.2	8.7
$G1^H$ + G3.1	24	353	-0.155	74.	0.074	62	62.8	5.7
$G1_H$ + G3.1	19	401	-0.224	91.7	0.044	41	188.	6.1
$G1_T$	13	341	-0.116	83.3	0.068	36	54.9	7.2
$G1_{H/T}$	9	395	-0.205	96.5	0.036	18	195.6	9.6
$G1_T$ + G3.1	22	381	-0.187	79.3	0.069	57	76.7	5.8
$G1_{H/T}$ + G3.1	18	419	-0.245	95.1	0.035	32	313.4	6.2

Here $G1_T$ = G1 - (33, 39); $G2_H$ = G1 - (1, 17, 42, 30); and G3.1 = (8, 12, 18, 21, 27, 31, 37, 41, 43). V is percentage of explained variance, σ is standard deviation, d is standard deviation as a percentage of the response mean. Notice that the computed (experimental) F value is always above the 99% confidence level (theoretical).

when one eliminates the dubious hydrological data (question marks in Figure 1) and/or the data which do not fit the tectonic feature of the group they apparently belong to (circled numbers in Figure 1). This leads to subsets $G1_H$, $G2_H$ (dubious hydrological data removed), $G1_T$, $G2_T$ (data with tectonic misfit removed), and $G1_{H/T}$, $G2_{H/T}$ (both preceding types of data removed). Next, the proposed G3.1 and G3.2 subsets of G3 are added to G1, $G1_H$, $G1_T$, $G1_{H/T}$ and to G2, $G2_T$, $G2_H$, $G2_{H/T}$, respectively. The associated quantitative relationships, obtained by linear regression and significant at the 99% level (Fisher test), are summarized in Tables 4 and 5.

G1 basins: The following remarks can be made:

1. The global adjustment on G1 explains more than 81% of the data variability.

2. The substraction of the dubious hydrological data leads to a significant V increase (~12%) and thus reinforces the physical significance of the adjustment. Correlatively, the absolute value of the regression coefficients K, Do is significantly increased (Table 4).

3. The elimination of the data which present an apparent misfit with the G1 tectonic feature improves only slightly the variance V.

4. The addition of G3.1 to either G1 or $G1_H$ does not modify the previous statistical results. This stresses the fact that the G3 clustering is located in a neutral region of the graph.

5. The linear adjustments present (Table 4) a slope coefficient K ranging from 320 x 10^{-6} to 420 x 10^{-6} (10^{-3} yr^{-1}) and a clear departure from zero of the intercept coefficient Do which ranges progressively from -0.09 to -0.245 and is always significantly greater in absolute value than the standard deviation σ.

G2 basins: The following remarks can be made:

1. The statistical criteria (V, σ, d) show (Table 5) that these adjustments, although significant, are not as good as for G1.

2. Differently from G1, the improvement of V has mainly to be ascribed to the

TABLE 5. Regression Laws Ds=K.H+Do for Basins Associated With Old Orogenies

Group	Number of Basins	K, 10^{-3} yr^{-1}	Do, $m/10^3$ yr	V,%	σ, $m/10^3$ yr	d,%	Fisher Test Experimental	Fisher Test Theoretical
G2	15	74 x 10^{-6}	-0.02	66	0.031	74	25.3	6.7
$G2_H$	14	52	-0.009	69	0.019	60	26.7	6.9
$G2^H$ + G3.2	21	77	-0.029	65.1	0.028	84.	35.5	5.9
$G2_H$ + G3.2	20	54	-0.015	63.7	0.018	72.6	31.6	6.0
$G2_T$	13	83	-0.022	79	0.027	59	41.7	7.2
$G2_{H/T}$	12	61	-0.011	86.5	0.014	41	64.3	7.6
$G2_T$ + G3.2	19	86	-0.031	74.0	0.025	73.7	50.4	6.1
$G2_{H/T}$ + G3.2	18	63	-0.019	75	0.016	63.5	48.0	6.2

Here $G2_T$ = G2 - (26, 36); $G2_H$ = G2 (19); G3.2 = (2, 4, 5, 6, 28, 32); and $G2_{H/T}$ = G2 - (19, 26, 36). Same definitions for V, σ, d, and Fisher test as in Table 4.

removal of the data which are in tectonic misfit with G2 rather than to the elimination of the uncertain hydrological data.

3. As previously noted for G3.1 with G1 basins, the addition of G3.2 to G2 has no significant effect on the linear adjustments.

4. The slope coefficient K fluctuates between 83 x 10^{-6} and 63 x 10^{-6} ($10^{-3}/yr^{-1}$), and the intercept Do fluctuates between -0.029 and -0.011 $m/10^3$ yr and is on the order of the standard deviation σ. The linear adjustments, obtained for the following groupings $G1_{H/T}$+G3.1 and $G2_{H/T}$G3.2, are displayed in Figure 3.

Modeling of erosion/sedimentation (above sea level) versus relief. The quantitative relationships for both G1 and G2 between mechanical denudation rate Ds and H are Ds = K . H + Do, with Do < 0. The absolute value of Do is significantly greater (see Table 4) than the standard deviation σ for G1 basins while on the order of σ for G2 basins (Table 5). This means that, at least in the case of G1 basins, it exists in the evaluated denudation rate Ds, a negative component which suggests that the assumption of a pure erosion process acting down to the sea level, implicitly done in our first approach with Ds = K . H, is not supported by the data. Consequently, a sedimentation process acting above sea level may be invoked. For a given basin j, it then becomes necessary to have the following mass budget inside the basin:

$$Ms_j = Mer_j - Mall_j$$

between the eroded mass Mer_j and the deposited alluvium $Mall_j$, with

$$Mer_j = \rho \cdot Der_j \cdot A_j = \rho \cdot (K.H_j) \cdot A_j$$

$$Mall_j = \rho \cdot Dall \cdot A_j$$

where Der_j and Dall are the erosion and alluvial rates, respectively. Dall, being constant, has to be uncorrelated with H_j and A_j (notice that H and Ds in Table 3a are uncorrelated with A), and $Ds_j = Ms_j/\rho \cdot A_j = K \cdot H_j - Dall$ is in agreement with the computed values at the river mouth. This will be referred to as model I (Figure 4). However, this implies a homogeneous sedimentation throughout the basin. A continental sedimentation located essentially in the lowlands of the fluvial basins seems more realistic.

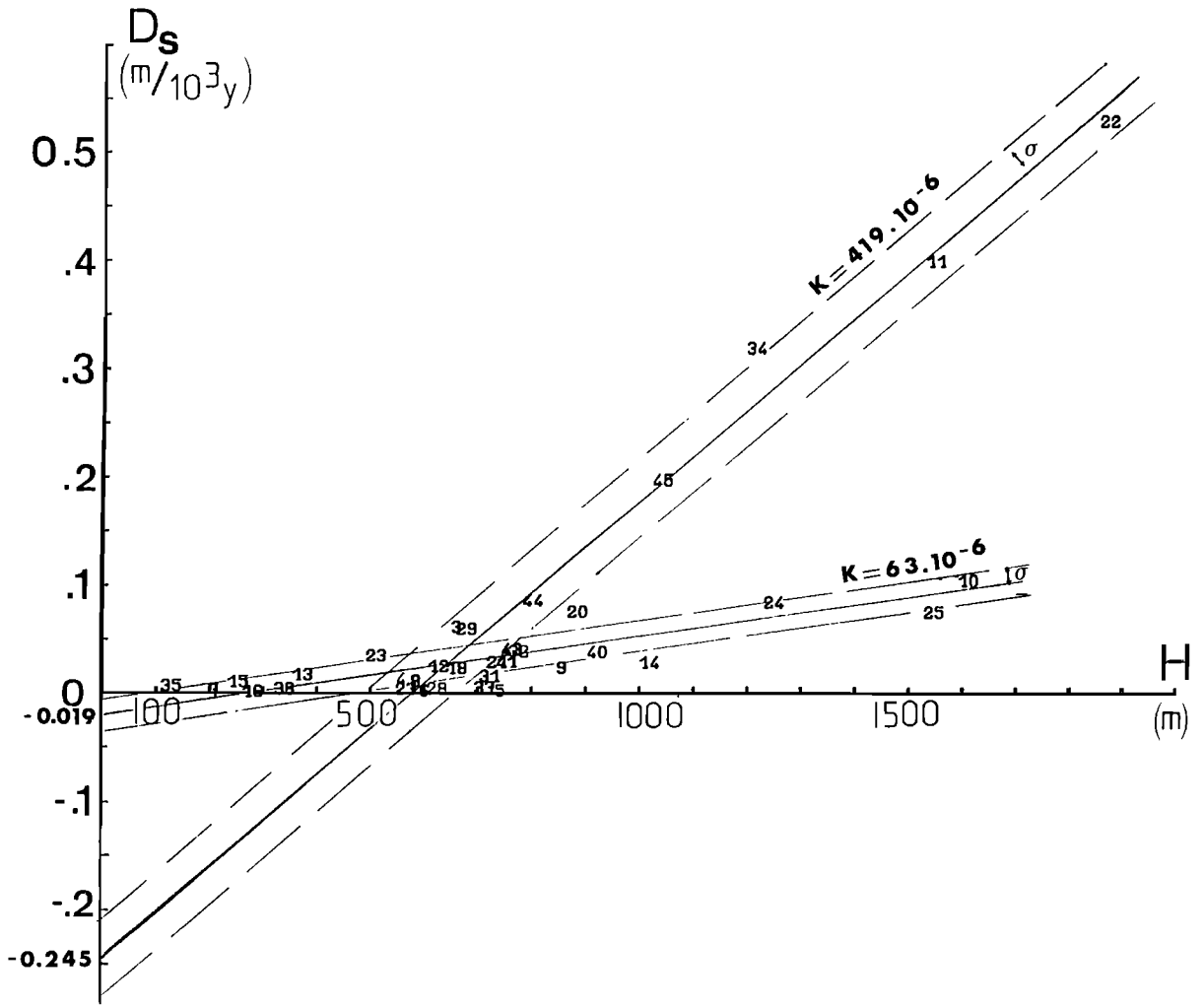

Fig. 3. Representation of the linear adjustments obtained for the proposed groupings $G1_{H/T}$+G3.1 and $G2_{H/T}$+G3.2 (see Tables 4 and 5) with their standard deviation interval: (1) $Ds = 419 \times 10^{-6} H - 0.245$, $\sigma = 0.035$ m/10^3 yr; and (2) $Ds = 63 \times 10^{-6} H - 0.019$, $\sigma = 0.016$ m/10^3 yr.

Then one can assess that a threshold in the river capacity is reached at some place without correlation to the mean elevation H_j. Beyond this threshold, the suspended sediment load is progressively deposited in agreement with a nonequilibrium state for the watersheds [e.g., Trimble, 1977, 1983]. We are thus driven to a simple model based on the following assumptions: (1) the erosional process prevails in the upper part of the basin Asup, (2) the sedimentation process is dominant in the lower part Ainf, and (3) in between, there may exist a transition zone where the two processes compete with each other.

In a first-order approximation, we reduce the transition zone to a fixed level Hc and thus consider only the first two zones, hereafter referred to as model II (Figure 4): (1) Below Hc, sedimentation occurs; then the alluvial mass is $Mall_j = \rho \cdot Dall \cdot Ainf_j$, where Dall is a mean alluvial rate for all the basins in the set, and $Ainf_j$ is the area below Hc, given by the hypsometric curve of the basin j. (2) Above Hc, we assume an erosion process according to the previous analysis; then $Mer_j = \rho \cdot K \cdot H'_j \cdot Asup_j$, where H' is the mean height above Hc and $Asup_j$ the relevant area.

Consequently, $Ds_j = K \cdot H'_j$

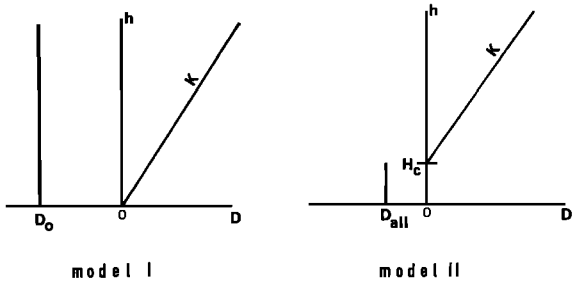

Fig. 4. Schematic representation of model I (erosion/sedimentation from basin top to sea level) and model II (erosion above Hc; sedimentation below Hc).

$. (Asup/A)_j - Dall . (Ainf/A)_j$, where K and Dall are the two coefficients to be fitted. This model will be successful if there exists a value of the parameter Hc with yields a null intercept with a small standard deviation .

This model is successively applied to the groupings $G1_T + G3.1$ and $G1_{H/T} + G3.1$ with Hc starting from 100 m and increasing with a 100-m step, which is the sampling step in our hypsometric curves. As Hc increases, the negative intercept coefficient D'o approaches zero and even becomes positive for Hc = 700 m (Table 6). It is worthwhile to note that, although the individual slope for each basin may be somewhat modified when Hc varies, the global slope K of the set is very stable and stays around 420×10^{-6} (10^{-3} yr^{-1}) (see Table 6 and Figure 5) in relation with significant and stable statistical criteria (V, σ, d). For the critical level Hc = 600 m, the intercept D'o is close to zero and clearly inside the standard deviation interval; the slope K is equal to 415×10^{-6} (10^{-3} yr^{-1}). We establish (Figure 5), for this Hc value, the graph

$$Ds_j + Dall . (Ainf/A)_j = f (H' . Asup/A)_j$$

and give in Table 7, for each basin of the set, the measured mass of sediment at the river mouth Ms, the ratios Mdep/Ms, Mer/Ms, and Mdep/Mer where Mdep and Mer are the alluvial deposited mass below Hc and the total eroded mass, respectively. In spite of the partial failure of the model in some particular cases, because of its roughness (e.g., the theoretical Ms estimate is much weaker than the observed one for Huangho basin), these results demonstrate that there is a wide variability in the sediment storage process. However, this process is usually far from negligible. The time constant of erosion $\tau = 1/K$ is also calculated for each basin; this shows that it takes between 1.3 and 4.6 m.y. in order to reduce the basin relief to 37% of its

TABLE 6. Determination, for the Basins Belonging to $G1_{H/T}+G3.1$, of Coefficients (K,Dall) in the Bilinear Regression Law: $Ds_j = K.H'_j.(Asup/A)_j - Dall.(Ai/A)_j + D'o$ for Hc Ranging from 0 to 700 m

Hc, m	K, 10^{-3} yr^{-1}	Dall, $m/10^3$ yr	D'o, $m/10^3$ yr	V, %	σ, $m/10^3$ yr	d, %
			$G1_{H/T}+3.1$			
0	419×10^{-6}	0	-0.245	95.1	0.035	32.
100	420	0.1195	-0.192	95.4	0.035	32.5
200	418	0.0334	-0.163	94.9	0.037	34.
300	416	0.0531	-0.122	94.8	0.037	34.
400	417	0.0457	-0.094	94.6	0.038	35.
500	419	0.0635	-0.059	94.5	0.038	35.
600	415	0.1094	-0.011	94.6	0.038	35.
700	413	0.1369	-0.031	94.3	0.039	36.
			$G1_T+3.1$			
600	408.	0.0607	-0.009	81.8	0.066	55.

D'o is the closest to zero and within the σ interval for Hc = 600 m. For Hc = 600 m, the determination of K and Dall is also given for the group $G1_T+G3.1$, in which the uncertain hydrological data are not excluded.

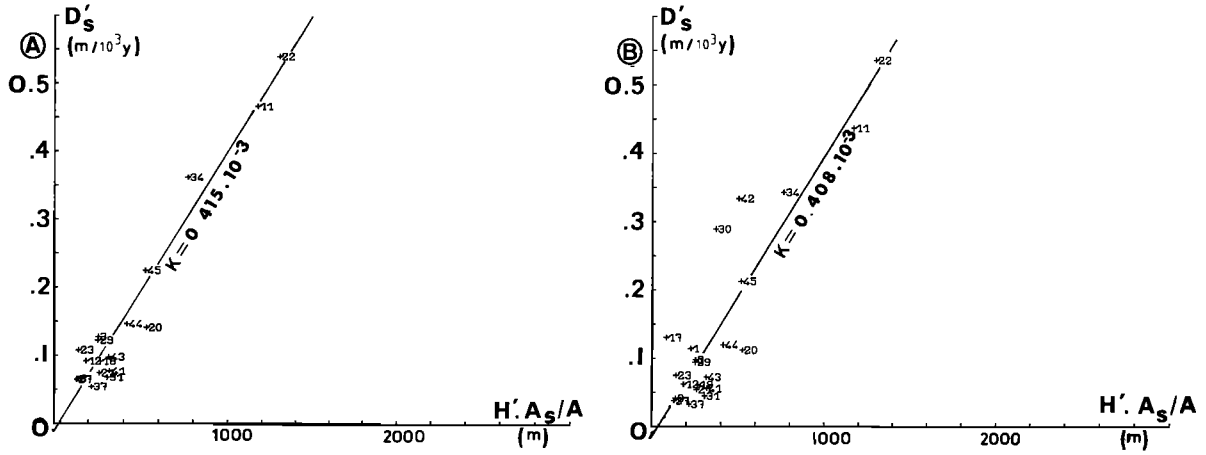

Fig. 5. Graph of D's = Ds + Dall . (Ainf/A) versus (H' . Asup/A) with Hc = 600 m, for basins belonging to (a) $G1_{H/T}$+G3.1 and (b) $G1_T$ + G3.1.

initial value (to preserve 10%, it takes between 3. and 10.5 m.y.); it is to be noted that these values lie between the estimates derived, at local scale, from the results of Ruxton and McDougall [1967] and, at regional scale, from those of Ahnert [1970].

For G2 basins, this analysis does not stand; as Hc increases, the initial adjustment Ds = K . H is destroyed, and

TABLE 7. Ratios Between Deposited Mass Mdep, Eroded Mass Mer, and Suspended Mass at the River Mouth Ms Obtained With Model II

	River	10^6 Ms, t/yr	Mdep/Ms	Mer/Ms	Mdep/Mer	10^6 C1, years	10^6 C2, years
1	Amazon	900.	0.87	1.87	0.47	2.01	4.62
3	Mississippi	500.	0.60	1.60	0.37	2.63	6.04
8	Amour	52.	2.81	3.81	0.74	3.44	7.92
11	Ganges/ Brahmaputra	1670.	0.09	1.09	0.08	2.67	6.14
12	Mackenzie	100.	1.50	2.50	0.60	3.03	6.97
17	Orinoco	210.	0.58	1.58	0.37	0.67	1.53
18	Tigris/ Euphrates	53.	1.66	2.66	0.62	4.43	10.19
20	Mekong	160.	0.48	1.48	0.33	4.74	10.90
21	Yukon	60.	0.87	1.87	0.47	4.88	11.22
22	Huangho	1080.	0.01	1.01	0.01	2.42	5.56
23	Danube	67.	1.18	2.18	0.54	1.91	4.39
27	Kolyma	6.	9.30	10.30	0.90	3.54	8.13
29	Si Kiang	69.	0.59	1.59	0.37	2.70	6.22
30	Irrawaddi	265.	0.13	1.13	0.11	1.28	2.95
31	Indigirka	14.	1.84	2.84	0.65	6.94	15.96
34	Magdalena	220.	0.07	1.07	0.07	2.23	5.12
37	Yana	3.	5.43	6.43	0.84	6.84	15.73
41	Rio Negro	13.	0.91	1.91	0.48	5.77	13.27
42	Hungho	130.	0.06	1.06	0.05	1.51	3.47
43	Rhone	10.	0.79	1.79	0.44	4.40	10.12
44	Pô	15.	0.39	1.39	0.28	3.49	8.03
45	Susitna	25.	0.08	1.08	0.07	2.45	5.64

C1 and C2 are time constants to reduce the initial basin relief to 37% and 10%, respectively.

there is no critical value Hc below which the sedimentation process can be concentrated. However, the adjustment, proposed for $G2_{H/T}$, which is statistically the most significant, has a negative intercept Do and presents a null intercept for a critical level H = 300 m below which one should expect some sedimentation process to act. As the value of the negative intercept is on the process of the standard deviation σ = 0.014 m/1000 yr, we conclude that this adjustment is not physically meaningful and that it should go through the origin. The extremely low Ds values, noted from some basins (5, 6, 7, 16, 27, 37) may be responsible for this shift. Consequently, one prefers to consider these basins separately and to derive for individual time constants.

These results indicate that, for drainage basins associated with active orogenies, sediment storage is a widely variable mechanism from one basin to another, in contrast to the erosion process, which presents a more global behavior. However, the critical threshold Hc ~ 600 m appears to be a constant feature in the sedimentation process of these basins.

INTERPRETATION

Given the wide variability in terms of climatology and vegetation cover encountered inside the different drainage basins, these results emphasize the fact that the relief and, through it, the acting tectonics transcend the external causes and remain the major controlling factor of continental denudation in large drainage areas.

However, as the time of evolution of the drainage basin, estimated from the age of the main associated orogeny, increases, the relation between denudation rate and relief differs and evolves according to the following scheme:

1. For basins linked to recent orogenies, belonging to the alpine cycle (e.g., Himalayas, Andes, Alps), it is necessary to call for sedimentation. Two relations, based on two different physical models (Figure 4), present an equal statistical performance and can be alternatively proposed. In both models, erosion is proportional to elevation; but in model I the lowest level of erosion is the sea level while in model II it is the 600-m level. Besides, the sedimentation process covers with a uniform spreading the whole basin area in model I while it is restricted to the area between 0 and 600 m in elevation for model II. The two models lead to about the same erosion time constant but while with model I, one obtains a negative intercept which implies a global sedimentation process all over the basin at a uniform rate of about 190-250 m/m.y., model II leads to a uniform sedimentation, restricted to the portion of basin below 600 m, with a rate of 60-110 m/m.y. Both this critical level Hc and the magnitude of the deposition are in agreement with data concerning the foreland basins [Gibbs, 1967; Beaumont, 1981]. On one hand, in the case of the Amazon basin, 85% of the sediment production comes from the Andes, representing 12% of the total basin surface [Gibbs, 1967]. A glance at the hypsometric curve of the Amazon basin (Figure 6) shows that this corresponds to the portion of the surface above 600 m and thus locates this threshold at the Piedmont of the orogenic belt. On the other hand, cross sections of the Alberta basin [Beaumont, 1981, Figures 5 and 6] lead from the stratigraphic record to sedimentation rates around 70 m/m.y., in better agreement with the estimate obtained from model II than that from model I, which ranks too high. However, concerning the erosion process, the two models provide essentially the same regression coefficient, leading to close erosion time constants on the order of 2.5 m.y. The mean elevation of these "young" basins is 810 m.

2. For basins related to older orogenies such as Hercynian and Caledonian, model II is no longer valid, and model I leads to relationships Ds = K . H + Do, given in Table 5, where the negative intercept on the order of the standard deviation is not significant. One then infers there is no active process of sedimentation inside the basin, i.e., above sea level, at this stage of its evolution, erosion acting in the whole basin, but at a much reduced pace, characterized by a time constant on the order of 25 m.y.. However, the mean elevation of these basins, with the exception of some very old basins considered below, is 850 m and thus is not substantially different with respect to the preceding group. Nevertheless, the mean elevation taken here as the relief variable may be inadequate to discriminate

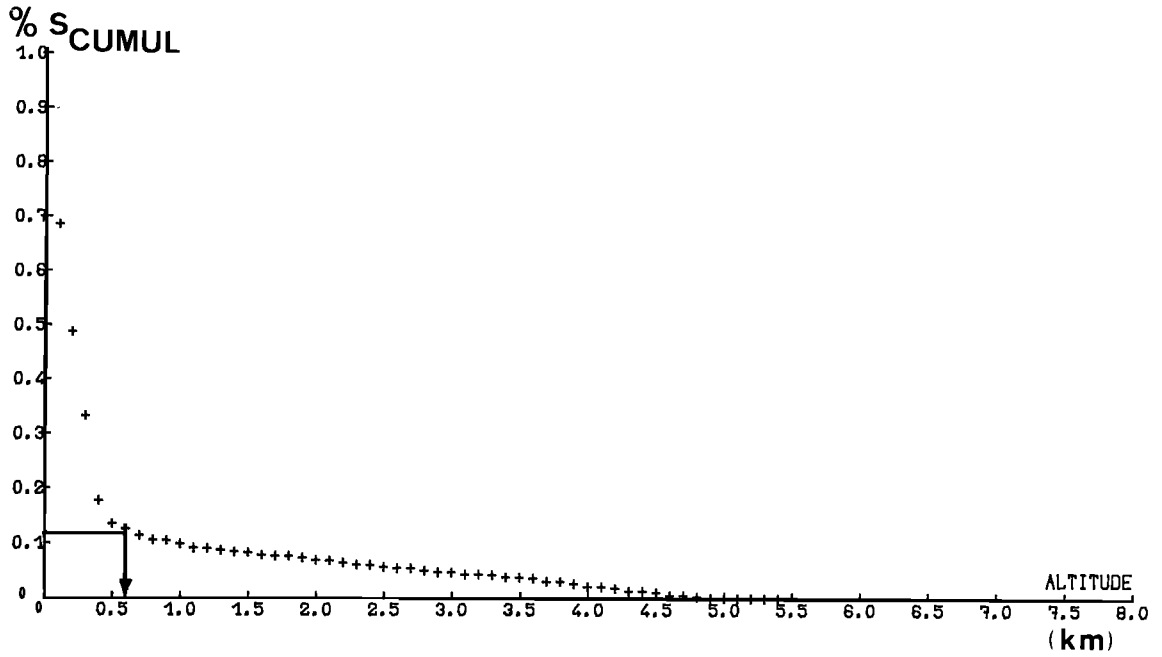

Fig. 6. Hypsometric curve of the Amazon basin (% S cumul is the percentage of cumulated surface above a given elevation level).

between different morphologies such as, for instance, the following two extreme ones: (1) a rugged topography, localized in a restricted portion of the total basin area, and (2) a smooth topography spread over the whole basin area. Such a discrimination would be possible in terms of slope distribution.

3. Finally, among this second group, there exist some large basins, associated with very old orogenic events and located in stable cratonic areas which appear as the tail part of the distribution in the basin evolution history. This subset of basins present very weak denudation rates, a lower global mean elevation (H = 500 m), and much longer erosion time constants (50-300 m.y.) with a larger dispersion than the preceding groups. Although a part of this dispersion may arise from the relatively more important uncertainty on these estimates, it may also mean that these basins represent the ultimate fate of very old remnant orogenies.

These results can be interpreted in the light of the model proposed by Beaumont [1981] for the formation of the foreland basins. In such an interpretation, the first time constant of erosion we obtain (2.5 m.y.) might correspond to the first phase of the orogeny when the downward flexure of the continental lithosphere occurs in response to passive loading by supralithospheric mass loads (Figure 7) and increases the slope between the mountain belt and the continental basement. This results in high denudation rates producing the infilling of the trough with associated subsidence. This first phase lasts as long as a significant tectonic input persists.

The second time constant (25 m.y.) corresponds to the weaker erosion process which occurs once the tectonic episode has ceased. Then the mean slope along which sediments are transported by the drainage network has been substantially reduced due to the previous development of foothills by infilling of the trough. Consequently, the erosion process works with less efficiency but on a larger spatial scale, progressively pushing the process of sedimentation inside the basin downward and even out of the basin, i.e., below sea level. The lack of intermediate values of the denudation rate Ds, noted in Figure 3, between the two distributions suggests that the transient between the two regimes occurs with a short time constant (i.e., on the order of 2.5 m.y.) so that the probability of presently detecting this transition phase is low.

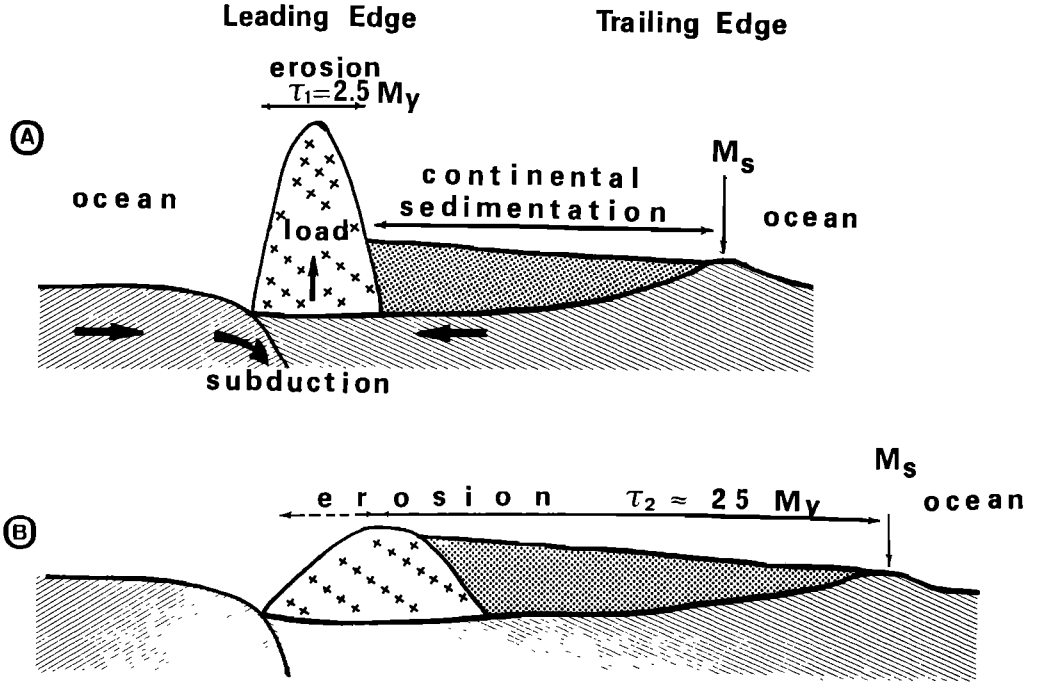

Fig. 7. Schematic cartoons showing the two kinds of basins found in this study and the corresponding associated erosion/sedimentation processes: (a) basin associated with young orogeny (the ocean-continent collisional tectonic context is considered here) and (b) basin associated with old orogeny. Note: Figures 7a and 7b can be seen as the major successive stages in the temporal evolution of a given basin.

One must notice that just after the tectonic phase has ceased, the mean elevation of the basin topography may be nearly unmodified while the associated denudation rate Ds is drastically reduced.

Finally, the very long time constants would correspond to a more widespread and passive mechanism of diffusion both enlarging the basin-eroding part and lowering the mean relief.

However, in the proposed scenario, one cannot exclude a global "tectonic" uplift at the basin scale, increasing the basin mean elevation without significantly affecting the denudation rate, derived from the global basin sediment budget.

During the first phase of the orogeny, the supracrustal load, in the framework of a thrusting mechanism, migrates toward the interior of the continental plate because of the convergent plate tectonics motion; as a consequence, the width of the orogenic belt and the size of the basin are both increased. Observational evidence for this is seen in the southern part of the Pyrenees [Labaume et al., 1985] where the rate of progradation of the sediment layers in the foreland basin is on the order of (or just larger than) the rate of migration of the responsible load, which is around 3.5 mm/yr. This implies a certain variability in the width of the belt, and the more recent an orogenic event is, the shorter the characteristic size of the belt must be. As a first approximation, we define the characteristic size of a belt as the square root of the basin surface above the threshold Hc = 600 m for recent orogenies and of the total basin surface for old orogenies; these values are plotted versus the erosion time constants in Figure 8. Our above prediction is globally checked, at least for basin associated with Alpine orogenies. Alpine and Himalayan belts present the shortest characteristic widths, followed by the part of the Andes corresponding to the Amazon basin, and then the Rockies associated with the Mississippi basin in agreement with the increasing age of the Himalayan, Alpine, and Nevadian orogenic phases. Accordingly, the approximate

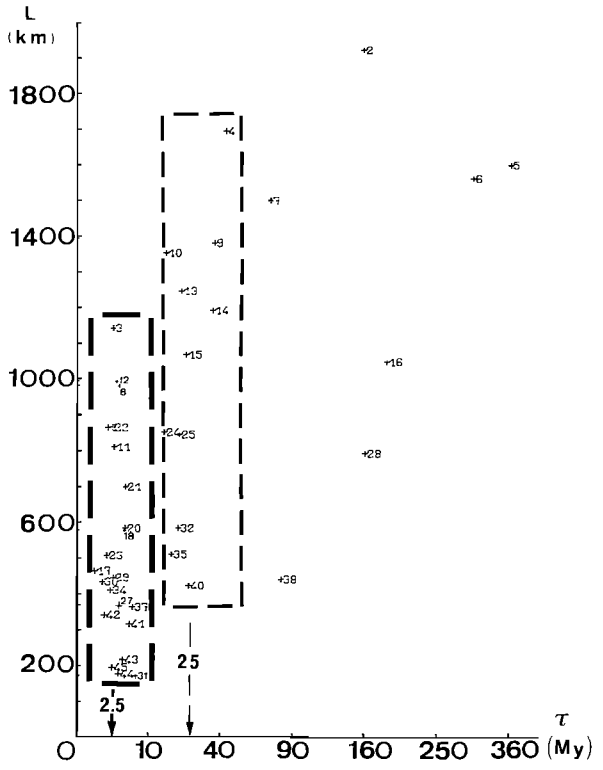

Fig. 8. Characteristic size L of an orogenic belt versus the obtained erosion constant τ for every drainage basin. Two groupings are seen around τ_1 = 2.5 m.y. and τ_2 = 25 m.y.; the vertical spreading displays the variability in the belt width; the values scattered toward very long τ values, associated with increasing basin sizes, hint at the existence of a passive diffusion mechanism in large-scale erosion processes.

characteristic lateral extent of an incipient orogenic belt would be around 200 km (Figure 8) and might range up to 1200 km in the case of the Rockies.

Besides, the short time constant 2.5 m.y. obtained with both models, needs an active tectonic input for several tens of millions of years, in order to preserve relief. As a matter of fact, without any tectonic input, the erosion process acts as a relaxation phenomenon of the relief, described by the solution (equation (4))

$$H(t) = Ho \exp(-t/\tau) \qquad \tau = 2.5 \text{ m.y.}$$

Taking into account a tectonic input leads us to introduce a driving term T in equation (3), and then one obtains

$$dH/dt = -H/\tau + T \qquad (5)$$

If one looks for a steady state regime, then dH/dt = 0, and the condition of stationarity for preserving the relief, H(t) = Ho, implies

$$T = Ho/\tau \qquad (6)$$

With a plausible value for a mountain relief Ho = 2500 m, equation (6) leads to a 1-mm/yr rate of uplift with τ = 2.5 m.y.. From radiometric dating and geothermobarometric data, such a rate is observed [Selverstone, 1985] in the southwestern Tauern Window, a region of the eastern Alps, over a long time period: 20-40 m.y. An independent estimate, indicating a 1.5-mm/yr uplift rate in the Himalayas during the last 2 m.y. is derived from comparison of the altitudes at which plant fossils of the Pleistocene are found presently [Ollier, 1981]. This uplift rate is also detected, at the much shorter time scale of 50 years, from leveling measurements in the Alps [Fourniguet, 1977; Gubler et al., 1981; Miller et al., 1982]. A corollary of the global scenario described above is that, in the case of an oceanic-continental plate convergence, since there is no sediment trapping on the leading continental edge because of the presence of the subduction zone, the sediment production on this side of the orogeny should be governed by erosion rates on the order of those obtained on the trailing edge (Figure 7), in the first phase of the erosion mechanism (time constant τ_1), before the tectonic input ceases and the sediment blanketing decreases the relief mean slope and thus slows down the erosion process. Even if the drainage networks are less developed on this side of the orogenies, they are more numerous and may provide us with, at least, a nonnegligible fraction of the world sediment delivery by big rivers flowing down mainly [Inman and Nordstrom, 1971; Potter, 1978] toward the trailing edge of the cratonic areas. Consequently, although these sediments are not accumulated and thus cannot be detected as they are swept down by the subduction zone, there is probably a significant production of continental sediment toward the ocean in this way, which contributes to the mantle recycling.

CONCLUSIONS

This worldwide analysis has revealed that the only major controlling factor of the continental denudation is the relief. However, one cannot exclude the effect of other environmental factors such as vegetation, climate, etc., at shorter spatial scales.

Many previous investigations have looked for a single time constant for the erosion process. This study has made obvious the existence of a wide spectrum of erosion time constants ranging from 2 m.y. up to 300 m.y. Nevertheless, these constants are not randomly distributed, and two preferential values are obtained. The first one, around 2.5 m.y., appears to be associated with active orogenies and implies a steady state for the tectonic input in contradiction with a classical assumption in geomorphology, stating that the input is instantaneous [e.g., Davis, 1899, 1909]. In addition, a continental sediment storage has been detected which indicates a nonequilibrium regime in the drainage process. The second time constant, around 25 m.y., is linked to "dead" orogenies. However, the scattering around this value (15-300 m.y.) is more important than in the previous case (Figure 8). With respect to these time scales, the tectonic input may be considered as instantaneous, in better agreement with Davis' interpretation. It is to be noted that, from the investigation of the relief distribution in regions located either on the Canadian shield or in Australia, such time scales have also been proposed [Stephenson, 1984, 1985a]. The associated lack of continental sedimentation suggests an equilibrium regime for the river transport.

It must be emphasized that these conclusions are based on quasi-instantaneous rates, derived from annual river sediment yields, and agree first with sedimentation estimates, derived from geological data provided by the foreland basin stratigraphy in Alberta [Beaumont, 1981], and second with uplift estimates, derived from petrographical [Selverstone, 1985] and leveling [e.g., Miller et al., 1982] measurements in the Alps.

This study appears as a preliminary step in which long wavelengths have been intentionally selected. As a matter of fact, the basin mean altitude chosen as the descriptive relief variable, is the output of a low-pass filter, a procedure justified by a worldwide statistical analysis. Some more information should be retrieved from shorter wavelengths, requiring the basin topography to be analyzed by means of other variables such as, for instance, relief slope or hypsometric distribution inside the drainage basin.

REFERENCES

Ahnert, F., Functional relationships between denudation, relief and uplift in large mid-latitude drainage basins, Am. J. Sci., 268, 243-263, 1970.

Beaumont, C., Foreland basins, Geophys. J. R. Astron. Soc., 65, 291-329, 1981.

Burchfiel, C., Continental crust, Sci. Am., 73, 1983.

Chorley, R. J., S. A. Schumm, and D. E. Sugden, Geomorphology, 605 pp., Methuen, New York, 1984.

Corbel, J., L'érosion terrestre, étude quantitative (méthodes-techniques-/ résultats), Ann. Geogr. J., 73, 385-/ 412, 1964.

Davis, W. M., The geographical cycle, Geogr. J., 14, 481-504, 1899.

Davis, W. M., Geographical Essays, Ginn., Boston, Mass., 1909.

Encyclopedia Brittanica, Table p. 276; maps, pp. 144, 142, 143, Atlas, 1969 .

Food and Agriculture Organization, F.A.O. flisheries, Circ., 134, 1971.

Fourniguet, J., Mise en évidence des mouvements néotectoniques actuels verticaux dans le sud-est de la France par la comparaison de nivellements successifs, paper presented at 5ème Réunion An. Sci. Terre, Rennes, 1977.

Gibbs, R. J., The geochemistry of the Amazon river system, The factors that control the salinity and composition and concentration of suspended solids, Geol. Soc. Am. Bull., 78, 1203-1232, 1967.

Gubler, E., H. G. Kahle, E. Klingele, St. Mueller, and R. Olivier, Recent crustal movements in Switzerland and their geophysical interpretation, Tectonophysics, 71, 125-152, 1981.

Holeman, J. N., The sediment yield of major rivers of the world, Water Resour. Res., 4, 737-747, 1968.

Holland, H. D., The Chemistry of the Atmosphere and Oceans, 351 pp., Wiley and sons, New York, 1978.

Inman, D. L., and C. E. Nordstrom, On the tectonic and morphologic classification of coasts, J. Geol., 79, 1-21, 1971.

Institut Géographique National, world map, scale 1:10 000 000, Mercator Projection, Paris, France, 1968.

Jansen, J. M. L., and R. B. Painter, Predicting sediment yield from climate and topography, J. Hydrol., 21, 371-/380, 1974.

Judson, S., and D. F. Ritter, Rates of regional denudation in the United States, J. Geophys. Res., 69(16), 3395-3401, 1964.

Labaume, P., M. Seguret, and C. Seyre, Evolution of a turbiditic foreland basin and analogy with an accretionary prism: Example of the Eocene-Pyrenean basin, Tectonics, 4(7), 661-685, 1985.

Langbein, W. B., and S. A. Schumm, Yield of sediment in relationq to mean annual precipitation, EOS Trans. AGU, 39, 1076-1084, 1958.

Lisitzin, A. P., Sedimentation in the world ocean, Spec. Publ. Soc. Econ. Paleont. Mineral., 17, 218 pp., 1972.

Meade, R. H., and R. S. Parker, Sediment in rivers of the U.S.A., National Water Summary 1984, U.S. Geol. Surv. Water Supply Pap., 2275, 1985.

Meybeck, M., Total mineral dissolved transport by world major rivers, Hydrol. Sci. Bull., 21, 265-284, 1976.

Meybeck, M., Les fleuves et le cycle géochimique des sédiments, Thèse d'Etat, Paris, 1985.

Miller, H., St. Mueller, and G. Perrier, Structure and dynamics of the Alps, in Alpine-Mediterranean Geodynamics, Geodyn. Ser., Vol 7, Edited by H. Berckhemer and K. Hsü, pp. 175-203, AGU, Washington, D.C., 1982.

Milliman, J. D., and R. H. Meade, World-/wide delivery of river sediment to the oceans, J. Geol., 91, 1-21, 1983.

National Center for Atmospheric Research, global 10 arc min elevation data map, Boulder, Colo., 1982.

NEDECO, River Studies and Recommendations on Improvement of Niger and Benue, 1000 pp., North-Holland, Amsterdam, 1959.

Ollier, C. D., Some regional examples, in Tectonics and Landforms, Geomorphol. Texts, Vol. 6, Clayton, p. 288, Longman Inc., New York, 1981.

Peters, J. J., Discharge and sand transport in the brailed zone of the Zaire estuary, Neth. J. Sea Res., 12, 273-292, 1978.

Potter, P. E., Significance and origin of big rivers, J. Geol., 86, 13-33, 1978.

Ruxton, B. P., and I. McDougall, Denu/-dation rates in northeast Papua from potassium-argon dating of lavas, Am. J. Sci., 265, 545-561, 1967.

Schumm, S. A., The evolution of drainage basin systems and slopes in badlands at Perth Amboy, New Jersey, Geol. Soc. Am. Bull., 67, 597-646, 1956.

Schumm, S. A., The disparity between present rates of denudation and orogeny, U.S. Geol. Surv. Prof. Pap., N° 454-H, 454-511, 1963.

Selverstone, J., Petrologic constraints on imbrication, metamorphism, and uplift in the SW Tauern Window, Eastern Alps, Tectonics, 4(7), 687-704, 1985.

Stephenson, R. S., Flexural models of continental lithosphere based on the long-term erosional decay of topography, Geophys. J. R. Astron. Soc., 77, 385-/414, 1984.

Stephenson, R., and K. Lambeck, Erosion-/isostatic rebound models for uplift: An application to south-eastern Australia, Geophys. J. R. Astron. Soc., Vol. 82, 31-55, 1985a.

Stephenson, R., and K. Lambeck, Response of the lithosphere with in-plane stress: Application to central Australia, J. Geophys. Res., 90(B10), 8581-8588, 1985b.

Trimble, S. W., The fallacy of stream equilibrium in contemporary denudation studies, Am. J. Sci., 277, 876-877, 1977.

Trimble, S. W., A sediment budget for Coon Creek basin in the Driftless Area, Wisconsin, 1853-1977, Am. J. Sci., 283, 454-474, 1983.

Trimble, S. W., and S. W. Lundt, Soil conservation and the reduction of erosion and sedimentation in the Coon Creek basin, Wisconsin, U.S. Geol. Surv. Prof. Pap., 1234, 35 pp., 1982.

UNESCO, Discharge of selected rivers of the world, general and regime charac-/teristics of stations selected, Stud. Rep. Hydrol. 5, 1, 70 pp., 1972.

UNESCO, Discharge of selected rivers of the world, mean monthly and extreme discharges (1969-1972), Stud. Rep. Hydrol. 5, 3(2), 124 pp., 1974.

UNESCO, Discharge of selected rivers of the world, mean monthly and extreme discharges (1972-1975), Stud. Rep. Hydrol. 5, 3(3), 104 pp., 1979.

Walling, D. E., and B. W. Webb, Patterns of sediment yield, in Background to

Paleohydrology, edited by K. J. Gregory, pp. 69-100, John Wiley, New York, 1983.

Wilson, L., Variations in mean annual sediment yield as a function of mean annual precipitation, Am. J. Sci., 273, 335-349, 1973.

P. Pinet and M. Souriau, E.R. 234, GRGS/CNES, 18, Avenue E. Belin, 31055 Toulouse Cedex, France.

(Received May 27, 1987;
revised October 12, 1987;
accepted November 16, 1987.)